COMPARISON OF MECHANICAL PROPERTIES AND STRUCTURAL CHANGES OF CONTINUOUS BASALT AND GLASS FIBRES AT ELEVATED TEMPERATURES

MARTIN ČERNÝ, PETR GLOGAR, VIKTOR GOLIÁŠ*, JAKUB HRUŠKA*, PETR JAKEŠ**, ZBYNĚK SUCHARDA, IVANA VÁVROVÁ*

Institute of Rock Structure and Mechanics, V Holešovičkách 41, 182 09 Prague, Czech Republic
**Institute of Geochemistry, Mineralogy and Mineral Resources, Faculty of Science, Charles University, Albertov 6, 128 43 Prague, Czech Republic*
***MDI Technologies, Ohradní 61, 140 00 Prague, Czech Republic*

E-mail: glogar@irsm.cas.cz

Submitted August 15, 2006; accepted December 6, 2006

Keywords: basalt fibre, glass fibre, tensile properties, elevated temperature, crystallization, X-ray diffraction

The investigated commercially available continuous basalt fibres fall short of selected glass fibres in their elastic and plastic response to tensile load at elevated temperatures. The onset temperature of unlimited elongation equals approximately 580 and 640, or 840 and 700°C for the basalt or glass fibres, respectively. The best (R-glass) fibre retains its modulus up to 450°C and loses but 8 % of its room-temperature value at 600°C, while the basalt fibres reveal significant losses of modulus (10-13 %) even at 450°C. Behaviour of the basalt fibres may be affected by onset of crystallization, which was detected by X-ray diffraction after heat treatment to 750°C.

INTRODUCTION

Continuous basalt fibres (CBF) - a novel class of man made mineral fibres - possess good thermal and electric insulating properties. CBF (in form of filaments or fabrics) are suitable materials for flame retarding and other thermally loaded applications (e.g., fire blocking interliners in public transportation seatings and fire resistant panels [1] or high-temperature heat-insulating materials [2]). Some aspects of CBF utilization as reinforcement in composites were investigated for various types of matrix: concrete [3] or polymer (epoxy [4], polypropylene [5-7] or phenol-formaldehyde resin [8], [9]). Fibre-matrix interface properties were studied in various basalt fibre-polymer matrix systems in, e.g., [4] or [5]. Good thermal stability of CBF allows even utilizing their reinforcing function in fibrous composites manufactured by means of an additional heat treatment (e.g., pyrolysis of a suitable polymer matrix yielding a ceramic matrix composite [10]).

It is therefore desirable to investigate thermomechanical properties of CBF at elevated temperature because they can play a significant role in forming the microstructure and the resulting mechanical properties of composites. Quantitative knowledge of the tow shrinkage is important also for mastering the manufacturing technology of fibre-reinforced composites with a pyrolyzed matrix [10] because the length contraction can cause deformation of the moulded bodies. Tensile properties of basalt fibres at temperatures to 300°C were measured and discussed in [11].

In the present study, basic properties and tensile behaviour at elevated temperatures (modulus up to 500-600°C, elongation even higher) of two commercially available basalt fibre types are examined and their properties are compared to those of conventional glass fibres. X-ray diffraction was used to identify structural changes of the fibres after heat treatment to 650°C and 750°C. Prototypes of basalt fibres prepared in the MDI Technologies laboratory using microwave melting and drawing the fibre through ceramic bushings [12] are also included in the study.

EXPERIMENTAL

Materials

Four types of basalt fibre and two types of glass fibre listed in Table 1 were investigated. Chemical composition of the fibres B1, B2, G1, and G2 is given in Table 2 where also product sheet data are included if available. The content of SiO_2 was determined by gravimetric analysis, that of TiO_2, Fe_2O_3 and P_2O_5 by UV-visible spectrometry (Unicam UV500), FeO and Al_2O_3 content by volumetric analysis, and content of MnO, MgO, Na_2O, and K_2O by atomic absorption spec-

trometry using the Varian AA2240 apparatus. For the glass G2 the unidentified residue of 8.0 % was attributed to B_2O_3, which could not be detected by the available methods (reported content of B_2O_3 is 5 ÷ 8 % [15]). The chemical composition of prototype basalt fibres B3 and B4, obtained using electron microanalyser CamScan S4-Link ISIS 300 EXD, is given in Table 3.

In order to guarantee a standard tensile load during tensile measurements, actual cross-sections of the fibre tows were determined from microscopic observation of the metallographically polished specimens with filaments mounted perpendicularly to the polished surface. The microscope Nikon Optiphot-100 equipped with an Image Analysis system Lucia was used for measurement of filament diameters (the assumption of circularity of filament cross-sections was well fulfilled). First, an average filament cross-section was determined by measuring (at high magnification) diameters of 220 randomly chosen filaments from 3 tow specimens of each of the fibres B1, B2, G1, and G2. Then, the average number of filaments in each tow specimen was found by counting at low magnification. The total tow cross-section was estimated by multiplying the both average values (Table 4). Due to a specific nature of the filament bundles B3 and B4 the distribution of their filament diameters was not pursued in this study.

Table 1. List of the investigated fibres.

	Grade	Producer	Type of product
B1		Bazaltex [13]	CBF
B2		Kamennyj Vek [14]	CBF
G1	RC 10	S. Gobain Vetrotex [15]	R-glass
G2	RO 99	S. Gobain Vetrotex [15]	E-glass
B3		MDI [12]	basalt filament
B4		MDI [12]	basalt filament

The broadest distribution of filament diameters was established with the fibre B1 while the fibre B2 revealed a significantly narrower one (Figure 1). The fibre G1 (R-glass) possesses an extremely narrow distribution of filament diameters (Figure 2).

Apparatus

Tensile behaviour of fibre tows at elevated temperatures was measured at gauge length 25 mm using a universal testing machine INSPEKT 50 kN (made by Hegewald-Peschke, Germany) equipped with a high-temperature extensometer PMA-12/V7-1 (Figure 3) with resolution 1 μm (made by Maytec, Germany). Figure 4 presents the scheme of the tensile measurement. A special attention had to be paid to the tow "conditioning" prior to tensile loading, i.e., smoothing particular filaments so that as many of them as possible would get under tension during the tow loading. The procedure was especially crucial before measuring the modulus.

Table 3. Chemical composition of the investigated developmental fibres B3 and B4.

	B3	B4
	(%)	
SiO_2	46.47	51.55
TiO_2	1.38	2.67
Al_2O_3	13.54	12.95
Σ FeO	12.83	9.21
MnO	0.20	0.28
MgO	14.19	4.62
CaO	8.77	10.68
Na_2O	2.13	5.40
K_2O	0.38	1.99
P_2O_5	0.10	0.65

Table 2. Chemical composition of the investigated commercially available fibres.

	B1 measured (%)	B1 reported [13] (%)	B2 measured (%)	G1 measured (%)	G1 reported [15] (%)	G2 measured (%)	G2 reported [15] (%)
SiO_2	50.5	57.5	53.6	57.2	58 ÷ 60	53.5	53 ÷ 57
TiO_2	2.8	1.1	1.1	0.2	N/A	0.3	N/A
Al_2O_3	13.4	16.9	17.4	23.6	23 ÷ 25	13.6	12 ÷ 15
Fe_2O_3	5.4	9.5	4.7	0.3	N/A	0.2	0.5
FeO	8.4	N/A	4.4	0.4	N/A	0.2	N/A
MnO	0.2	N/A	0.1	0	N/A	0	N/A
MgO	4	3.7	4.1	5.8	14 ÷ 17	1.2	22 ÷ 26
CaO	8.9	7.8	8.5	8.8	14 ÷ 17	21.4	22 ÷ 26
Na_2O	2.9	2.5	2.6	0.4	N/A	0.5	< 1
K_2O	1.6	0.8	1.6	0.85	N/A	0.5	< 1
P_2O_5	0.3	N/A	0.2	0.2	N/A	0.1	N/A

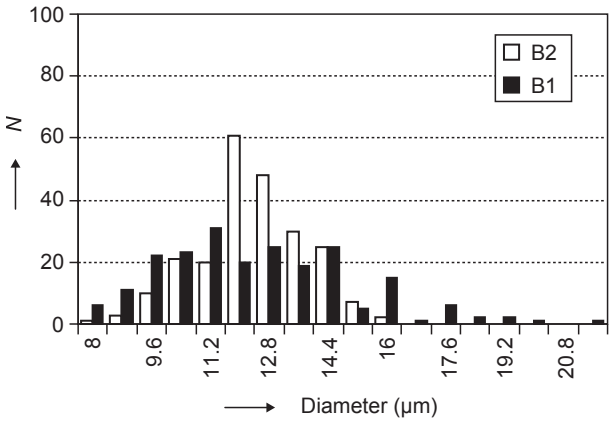

Figure 1. Distribution of filament diameters for fibres B1 and B2.

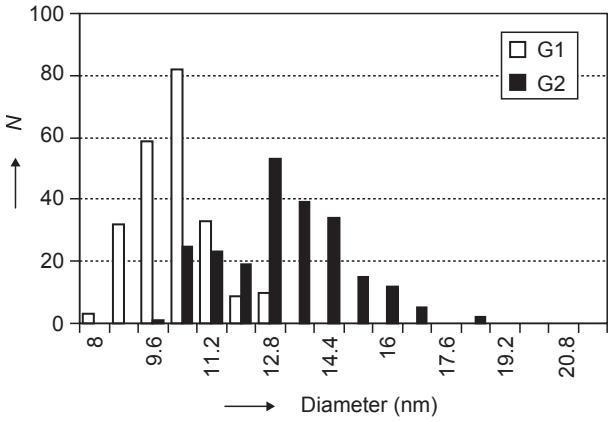

Figure 2. Distribution of filament diameters for fibres G1 and G2.

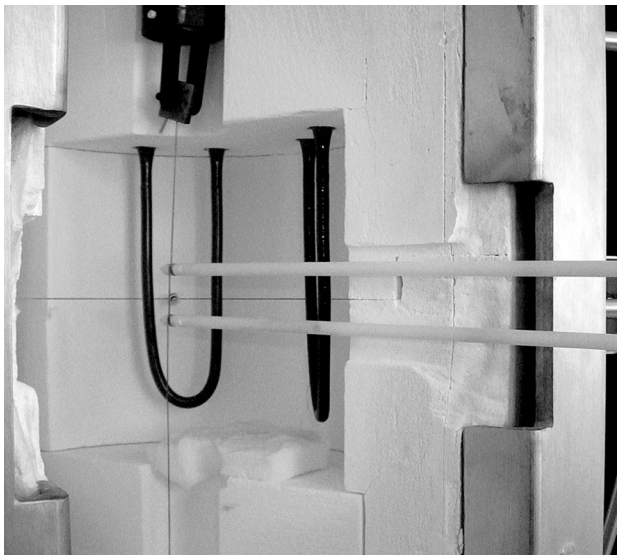

Figure 3. View of alumina rods transducing the tow elongation to the extensometer through a slot in insulation of the furnace (now open).

The X-ray diffraction (XRD) was used to detect structural changes, which may occur during thermal treatment of the investigated fibres. The measurements were carried out at the Institute of Geochemistry, Mineralogy and Mineral resources, Faculty of Science, Charles University, Prague. The fibres were studied by the powder diffraction method on the X`Pert Pro (PANalytical) diffractograph by CuKα radiation, with X`Celerator position sensitive detector. The samples were powdered in ethylalcohol and mounted onto silicon diffraction-free sample holder. The data were obtained in the continuous scanning mode between 20-100° (2θ) angles with step 0.05° and counting time 250 s. The obtained data were analysed using the HighScore software.

Table 4. Cross-sections of filaments and tows.

	Average filament cross-section (μm^2)	Average number of filaments in a tow	Total tow cross-section (mm^2)
B1	131.3 ± 61.5	1095 ± 8	0.143
B2	129.6 ± 29.3	974 ± 5	0.126
G1	89.9 ± 16.6	3980 ± 17	0.358
G2	145.5 ± 35.8	770 ± 3	0.111

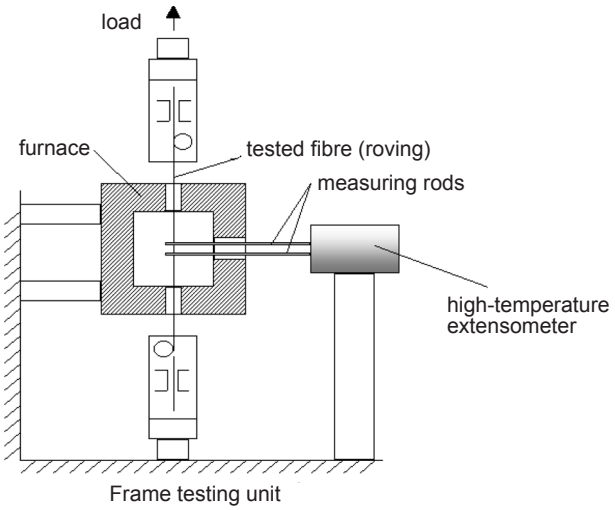

Figure 4. Scheme of the tensile measurement at elevated temperature.

RESULTS AND DISCUSSION

Tensile behaviour

Behaviour of the tows loaded by a tensile stress 10 MPa and heated at a rate 15 K/min is plotted in Figures 5 and 6. All fibres start to shrink slightly above 400°C, which is probably due to some plastic recovery originating in the manufacture process of the glassy material. On the other hand, the onset temperature of

unlimited elongation (creep) differs for particular fibres. It equals approximately 580, 640, 840, and 700°C for the fibres B1, B2, G1, and G2, respectively. For prototype fibres B3 and B4 the onset of creep takes place at approximately 550 and 590°C.

The investigated CBF do not equal standard glass fibres in their endurance under tensile load at elevated temperatures. It may be caused by a higher content of alkali oxides in the used purely natural raw material (see Tables 2 and 3).

Tensile modulus of the tows B1, B2, G1, and G2 was measured under low load at temperatures up to 500 or 600°C. Repeated mountings of the tows yielded slightly different values of modulus, ranging 70-80 GPa. Their temperature dependences, however, were very similar. For the sake of clarity, values of modulus E_T at temperature T were normalized to the room-temperature value E_{RT} and their ratio was plotted in the graph (Figure 7). Uncertainty of the plotted mean values is less than ± 0.02.

The G1 fibres retain their modulus completely up to 450°C and lose but 8 % of its RT value at 600°C. The fibres G2 and B2 are mutually similar: they lose 3-4 % of the RT modulus at 400°C and 8-10 % at 450°C. At 500°C the B2 seems to slightly outperform the G2 (loss 12% for B2 compared to 17% for G2). The fibre B1 exhibits a drop of 13 % already at 450°C. The overall pattern of the E (T) dependence corresponds to the established in Figure 5 superiority of the fibre G1 over the G2, B2 and B1 fibres in tensile properties at elevated temperatures.

Structural investigation

In order to reach a certain insight into the obtained results some structural characteristics of the fibres were acquired by XRD.

Amorphous glasses have a structure arranged in the so-called short range order, which applies to the closest adjacent atoms (e.g., in –Si–O–Si– chains) and no periodicity occurs over longer distances. This arrangement is expressed by a pair distribution function (PDF) and it is also present in silicate glasses and disordered materials [16]. In the XRD pattern the short range order is displayed as a broad (several degrees wide) flat maximum or increased background. These broad maxima were detected in both pristine (unheated) and thermally treated fibres to 650°C and 750°C (heating rate 50 K/h, hold 1 h). The main broad maximum in the B2, G1 and G2 fibres lies at a 1.44-1.45 Å distance while the adjacent, less intensive diffuse maximum occurs at 1.25 Å (Figure 8). The position of broad diffuse diffraction maxima is marked by arrows (samples B2, G1, G2). No changes in the position of these diffuse maxima were observed after thermal treatment to 650 and 750°C. On the other hand, no significant broad maximum was observed in the XRD pattern of the B1 fibre.

The basalt fibres B1 and B2 heat treated to 750°C revealed in their XRD patterns sharp diffraction maxima, which thus manifested presence of crystalline phases.

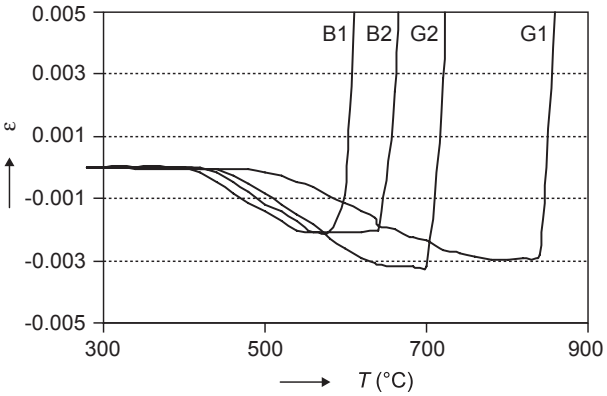

Figure 5. Elongation of the fibre tows B and G under constant tensile load at increasing temperature.

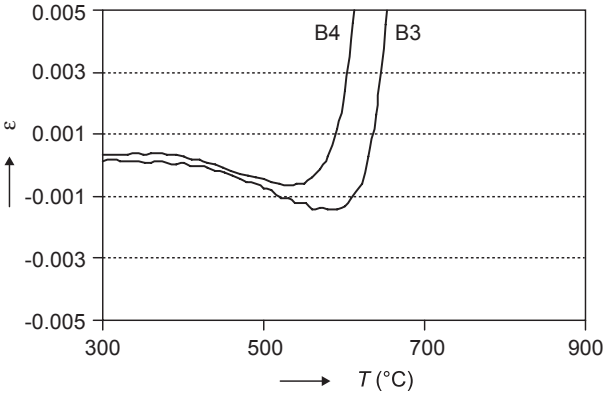

Figure 6. Elongation of the fibre tows B3 and B4 under constant tensile load at increasing temperature.

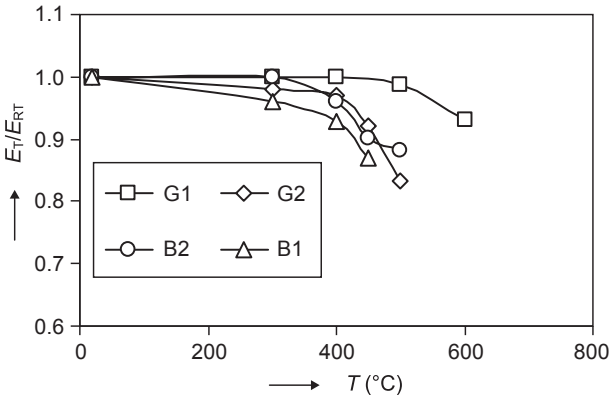

Figure 7. Temperature dependence of the normalized tensile modulus of the fibres B1, B2, G1 and G2.

These phases in the B1 fibre were identified as clinopyroxene and spinel (Figure 8a). In the B2 fibre only a spinel phase was identified (Figure 8b). In Figures 8a and 8b the position of diffraction maxima of the crystalline phases of clinopyroxene (cpx) and spinel (sp) in the B1 and B2 samples heated to 750°C is displayed.

In comparison with the PDF2 (Release 2003) ICDD database of the International Centre for Diffraction Data, clinopyroxene has an affinity to the diopside-hedenbergite-augite group. The phase with the spinel structure will be close to magnetite-magnesioferrite members. These results agree well with the observation [17] of similar synthetic materials. These authors found both mineral phases (magnetite and pyroxene) in iron-rich glasses during their crystallization process. In both G1 and G2 samples no crystalline phases were observed after thermal treatment.

The amount of crystalline phases in the studied basalt fibres is very low, certainly below 5 wt.%, but probably below 1 wt.%. The major portion of the material remains disordered.

Optical micro photographs of the composite with the B1 fibre and polymer-derived matrix heat treated to 650°C and 750°C are in Figures 9a and 9b. Due to matrix shrinkage during the thermal treatment the shape of (originally circular) fibre cross-sections is plastically distorted. A distinct difference between the fibre appearances is seen: after the treatment to 750°C the fibre cross-sections are finely granular while they are completely plain at 650°C.

An attempt was also made to monitor the inhomogeneity of the B1 fibre heat treated to 750°C also by scanning electron microscopy using the detection of backscattered electrons (BE). The latter may be used to

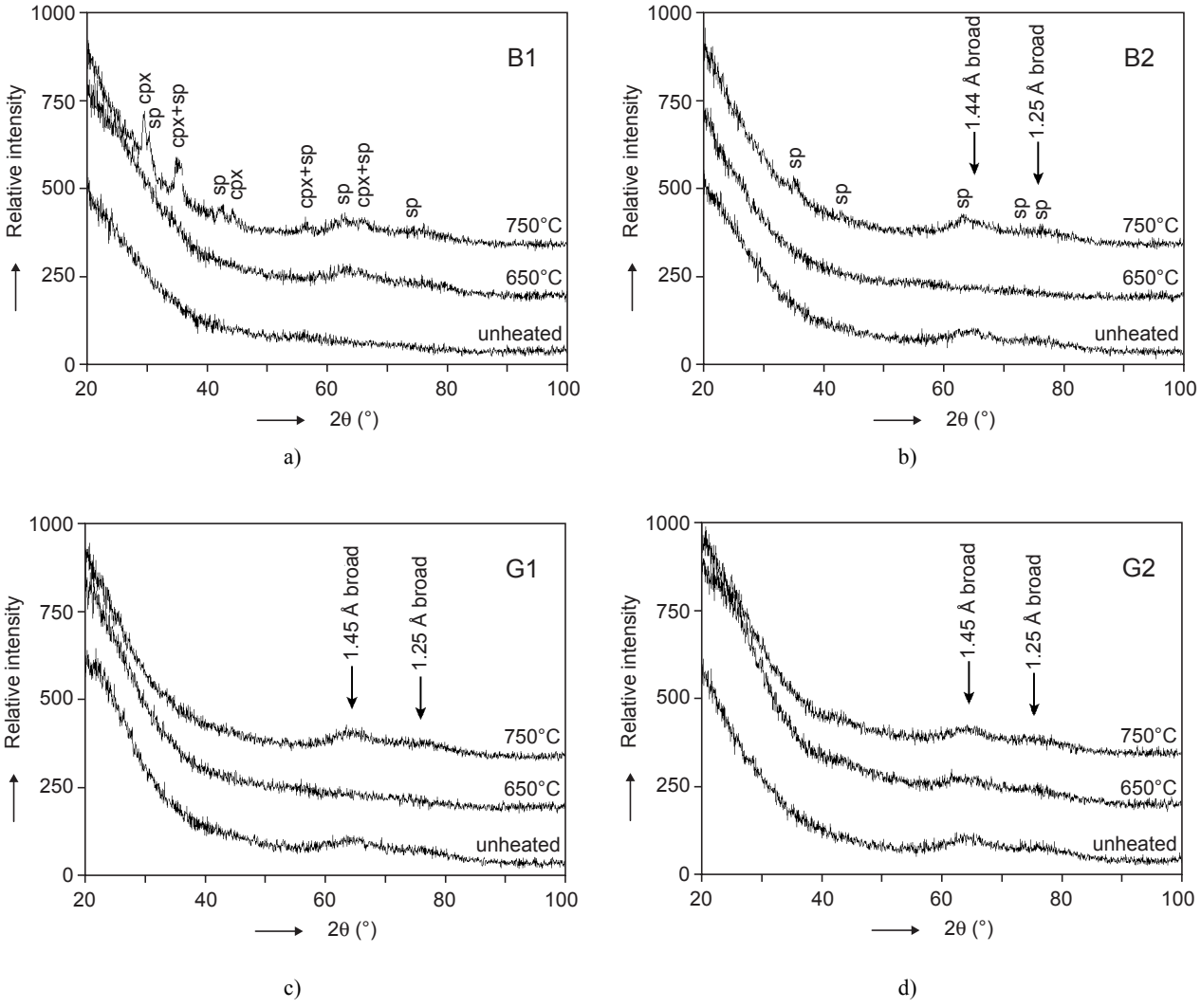

Figure 8. X-ray diffraction patterns of the pristine and heat-treated to 650 and 750°C basalt (a) and b)) and glass (c) and d)) fibres. Note: cpx - clinopyroxene, sp - spinel.

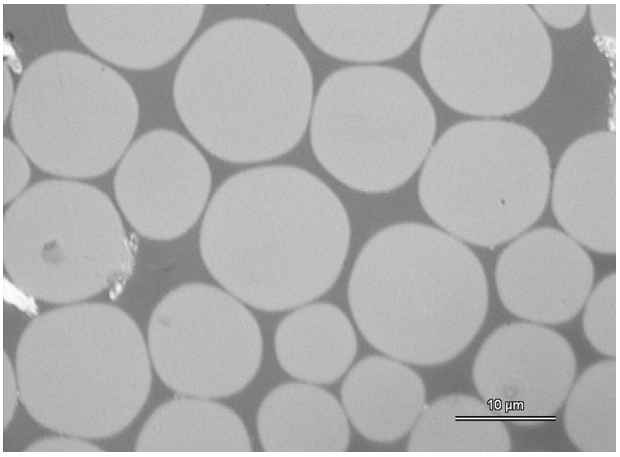

a)

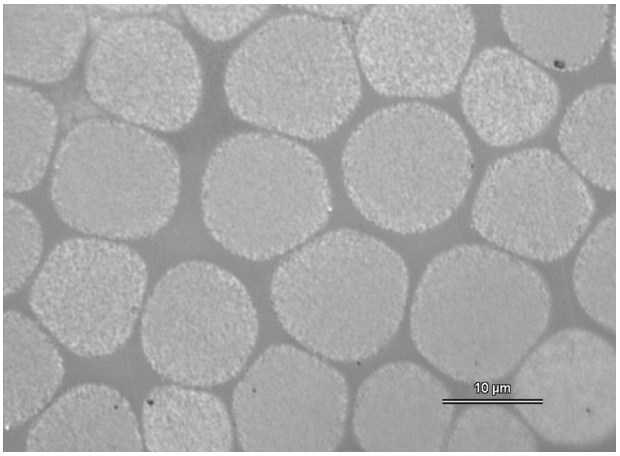

b)

Figure 9. Optical micro photographs of the cross-sections of the unidirectional composite with the B1 basalt fibres heat-treated to 650°C a) and 750°C b).

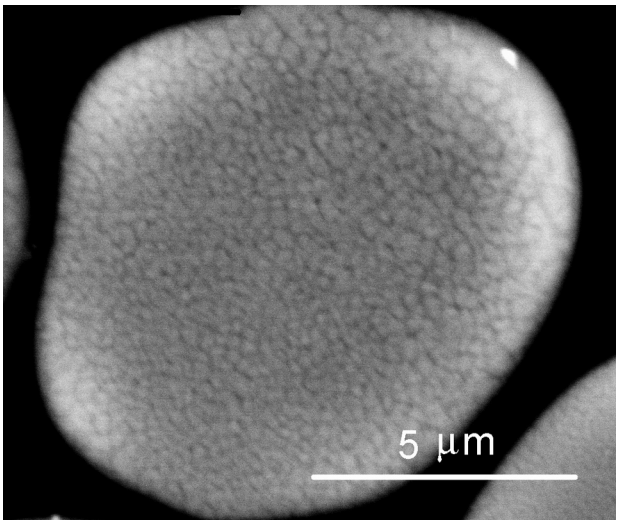

Figure 10. Backscattered electrons SEM image of a polished cross-section of the B1 basalt fibre heat-treated to 750°C in nitrogen.

detect contrast between areas with different chemical compositions (because of their greater energy, the BE can escape from much deeper regions of the sample than can secondary electrons). The BE image of the polished cross-section of the composite from Figure 9b is shown in Figure 10.

A distinct inhomogeneity (in a sub-micron size region) is visible, which probably stems from density fluctuations. These can be due to variations in either chemical composition or porosity. It may suggest more than an accidental coincidence with the fact that the B1 basalt fibre treated to 750°C reveals the most developed crystallinity among all the investigated fibres.

CONCLUSIONS

The investigated continuous basalt fibres resemble by shape and properties standard glass fibres. They are therefore suitable for reinforcing of composites with polymer matrix. In combination with a thermally stable matrix (see, e.g., [10]) they can serve up to 550-600°C in dependence on the fibre type. However, a significant loss of tensile modulus above 400 C must be taken into consideration. The onset temperature of deterioration of mechanical properties may be related to the detected crystallization, which does not occur with glass fibres up to 750°C. Though CBF lag behind glass fibres in thermal resistance their lower price makes them well competitive, not to mention their better alkali resistance. Moreover, the thermal resistance of CBF could be improved by suitable additives to the molten raw material, which is the route pursued currently by MDI Technologies [12].

Acknowledgement

The Czech Science Foundation supported this study through project No. 106/05/0817. Chemical analyses of basalt and glass fibres by P. Hájek, M. Malá, J. Švec, and J. Haloda and SEM photography by R. Procházka are gratefully acknowledged.

References

1. Nolf J.M.: Barrieres au feu en Basalte, www.basaltex.com.
2. Novitskii A.G.: Refract. Ind.Ceram. *45*, 144 (2004).
3. Sim J., Park C. and Moon D.Y.: Compos.Pt. B-Eng. *36*, 504 (2005).
4. Park J.M., Shin W.G. and Yoon D.J.: Compos.Sci.Technol. *59*, 355 (1999).
5. Matko S., Anna P., Marosi G., Szep A., Keszei S., Czigany T. and Posloskei K.: Macromol.Symp. *202*, 255 (2003).
6. Botev M., Betchev H., Bikiaris D. and Panayiotou C.: J.Appl.Polym.Sci. *74*, 523 (1999).

7. Bashtannik P. I., Ovcharenko V.G. and Boot Y.A.: Mech.Compos.Mater. *33*, 600 (1997).
8. Ozturk S.: J.Mater.Sci. *40*, 4585 (2005).
9. Artemenko S. E.: Fibre Chem. *35*, 226 (2005).
10. Černý M., Glogar P., Sucharda Z., Machovič V.: Ceramics-Silikáty *49*, 145 (2005).
11. Militký J., Kovačič V., Rubnerová J.: Eng.Fract.Mech. *69*, 1025 (2002).
12. Jakeš P., Burda M., Johnová R.: US Patent, 2004/0056026 A1.
13. www.basaltex.com
14. http://www.basfiber.com/en/roving.shtml
15. http://www.vetrotextextiles.com/pdf/E_R_and_D_glass_properties.pdf.
16. Proffen, T., Page K.L., McLain S.E., Clausen B., Darling T.W., TenCate J.A., Lee S.Y., Ustundag E.: Z. Kristallogr. *220*, 1002 (2005).
17. Pisciella P., Pelino M.: J.Eur.Cer.Soc. *25*, 1855 (2005).

SROVNÁNÍ MECHANICKÝCH VLASTNOSTÍ A STRUKTURNÍ ZMĚNY NEKONEČNÝCH ČEDIČOVÝCH A SKLENĚNÝCH VLÁKEN PŘI ZVÝŠENÝCH TEPLOTÁCH

MARTIN ČERNÝ, PETR GLOGAR, VIKTOR GOLIÁŠ*, JAKUB HRUŠKA*, PETR JAKEŠ**, ZBYNĚK SUCHARDA, IVANA VÁVROVÁ*

Ústav struktury a mechaniky hornin AVČR, V Holešovičkách 41, 18209 Praha 8
**Ústav geochemie, mineralogie a nerostných zdrojů, Přírodovědecká fakulta Univerzity Karlovy, Albertov 6, 128 43 Praha 2*
***MDI Technologies, Ohradní 61, 14000 Praha 4*

Studovaná komerčně dostupná nekonečná čedičová vlákna nedosahují vlastností vybraných skleněných vláken s hlediska elastické a plastické odezvy na tahové namáhání při zvýšených teplotách. Neomezené prodloužení nastává u čedičových vláken přibližně při 580 a 640°C, zatímco u vláken skleněných až při 840 a 700°C. Nejlepší skleněné vlákno (R-sklo) zachovává velikost tahového modulu pružnosti až do 450°C a při 600°C ztrácí jen 8% své nízkoteplotní hodnoty, zatímco čedičová vlákna vykazují podstatný pokles modulu (o 10-13%) již při 450°C. Chování čedičových vláken může být ovlivněno nástupem krystalizace, jež byla zjištěna rentgenovou difrakcí po tepelném zpracování na 750°C.